Highlights

- A new nanostructured TiO_2 film deposited on a stainless steel mesh was prepared
- The new supported photocatalyst was successfully reused several times.
- Identified by-products revealed minor differences between photocatalytic processes
- toxicity tests showed that few of them are useful for investigating CECs degradation

A new supported TiO$_2$ film deposited on stainless steel for the photocatalytic degradation of contaminants of emerging concern

S. Murgolo[1], V. Yargeau[2], R. Gerbasi[3], F. Visentin[3], N. El Habra[3],

G. Ricco[4], I. Lacchetti[5], M. Carere[5], M. L. Curri[6], G. Mascolo[1]*

(1) CNR, Water Research Institute, Via F. De Blasio 5, 70132 Bari, Italy.

(2) McGill University, Department of Chemical Engineering, University Street, Montreal, Quebec, Canada.

(3) CNR, Institute for Energetics and Interphases, Corso Stati Uniti 4, Padova, Italy.

(4) Regional Environmental Protection Agency, Via Oberdan 16, 70121 Bari, Italy.

(5) National Institute of Health, Department of Environment and Primary Prevent Unit Soil and Waste, Viale Regina Elena 299, Rome, Italy.

(6) CNR, Institute for Physical and Chemical Processes, Via Orabona 4, 70126 Bari, Italy

* Corresponding author. Tel.: +39 080 5820519; fax: +39 080 5313365.

e-mail address*: giuseppe.mascolo@ba.irsa.cnr.it (G. Mascolo).

Abstract

A new supported catalyst composed of a nanostructured TiO_2 films deposited on a stainless steel mesh (nanoTiO$_2$-SS) using the Metal Organic Chemical Vapour Deposition (MOCVD) technique was employed for the photocatalytic degradation of a mixture of contaminants of emerging concern. Results showed that under the oxidative conditions tested, the nanoTiO$_2$-SS catalyst had better performance in degrading the target contaminants than direct photolysis and photocatalysis using the conventional TiO_2 Degussa P25 catalyst. Specifically, the rate of removal of warfarin and trimethoprim obtained with the new catalyst was twice the one observed using TiO_2 Degussa P25 and approximately 1.6 times faster for metoprolol, carbamazepine and gemfibrozil. An evaluation of the electrical energy per order magnitude of removal (EE/O) confirmed the better performance of the new catalyst (24.3-31.8 kWh m^{-3} rather than 49.6-129 kWh m^{-3}) and that the performance is also compound-dependent. Toxicity tests revealed that some of them are really worth to be used for investigation of environmental effects of treated waters containing contaminants of emerging concern at µg L^{-1} level. Specifically, AMES Fluctuation Test, Fish Embryo Acute Toxicity and Growth Inhibition test by Green Alga were able to provide valuable results for an environmental assessment. On the other hand, *Daphnia Magna Straus* and Vibrio tests were not sensitive enough to the investigated samples.

2

1. Introduction

Research on various wastewater treatment technologies have demonstrated that conventional wastewater treatment plants (WWTPs), mainly based on physicochemical and biological processes, do not efficiently remove a wide variety of organic pollutants [1,2]. Pharmaceuticals and personal-care products (PPCPs), endocrine disruptor compounds (EDCs), illicit drugs, anticancer drugs, flame retardants, pesticides, perfluorinated compounds and other xenobiotic substances, are known to enter the wastewater network at concentrations in the $\mu g\ L^{-1}$-$ng\ L^{-1}$ range. The main sources of these contaminants in the wastewater and aquatic ecosystems are anthropic activities as well as from landfill leachates, runoff from agriculture, livestock and aquaculture [3-5]. The presence of these contaminants in the environment has been shown to cause long-term ecological effects such as loss of habitats and biodiversity, feminization of fish, development of microbiological resistance and accumulation in soil, plants and animals [6-8].

Organic pollutants classified as contaminants of emerging concern (CECs) consist of compounds that are not yet regulated and have no discharge limits but have raised concerns and are often on priority lists of various regulatory agencies. The relevance of addressing the problem of organic pollutants was taken into account by the Directive 2013/39/EU [9]. In addition, a watch list of 10 other substances was further defined by Decision 2015/495 on March 20, 2015.

Currently, significant research effort on wastewater treatment is aimed at finding effective technologies for CECs removal. In this contest, advanced oxidation processes (AOPs) based on the action of highly reactive and non-selective oxidants such as hydroxyl radicals (E^0=2.81 V) have been identified as promising technologies for degrading such compounds [10-13]. Numerous publications have drawn the attention to the AOPs like a technology applicable as pre-treatment of biological processes or post-treatment, namely tertiary treatment processes [14-16]. The integration of AOPs prior to biological treatment allows the production of a more biodegradable effluent that can be further treated by a cheaper and conventional biological process with shorter residence time

3

and reduced oxidant requirements in comparison to using AOPs as standalone processes. However, it is important to eliminate the oxidizing agents before any biological treatment, since they can inhibit the growth of beneficial microorganisms [17,18]. In this context, heterogeneous photocatalysis is an attractive AOP, due to absence of chemicals left at the end of the treatment that makes the process environmental friendly [19-21]. Irradiation of TiO_2 with photon having an energy equal or higher than TiO_2 band gap (3.2 eV for anatase, 3.0 eV for rutile and ~3.2 eV for brookite) promotes an electron from the valance band to conduction band (e_{CB}^-), and leaves an electronic vacancy or hole (h_{VB}^+) in the valance band. This hole is highly oxidative and rapidly reacts with surface sorbed organic molecules leading to their degradation. Hydroxyl radicals are also generated through the oxidation of adsorbed water molecules or hydroxyl ions [22, 23], further contributing to the degradation of the contaminants. The bench-mark catalyst, namely TiO_2 Degussa P25, has to be employed as a aqueous suspension although several studies investigated the immobilisation of the catalyst onto numerous substrates in order to facilitate recovery and reuse of the catalyst [24-26]. This approach is required to obtain a scalable and economically viable process. However, the efficiency of treatment in such heterogeneous reactive system relies heavily on the adsorption of reactants at the active sites of the catalyst surface and the immobilization of the catalyst inevitably leads to a loss of photocatalytic efficiency by reducing the active surface. In this context, one of the innovative aspects of this work is the use of nanostructured catalysts. TiO_2 nanoparticles (NPs) after immobilization allows to overcome such a problem because of their high surface-to-volume ratio leading to a higher active sites density to be used for adsorption. Also, another benefit of the nano-size of NPs is that the photo-generated charges can easily migrate toward the surface of the catalyst leading to a lower probability of bulk recombination [27-28]. The immobilization of the NPs TiO_2 also prevents NPs from leaching into water, thus strongly limiting the potential threat associated to dispersion of NPs into the environment.

The mineralization levels achieved for most of these oxidative processes operated at practical operating conditions have been determined as being quite low, leading to a growing interest in the detection and identification of the transformation products resulting from the application of AOPs [29-30] as well as in the evaluation of the residual toxicity by monitoring responses in test organisms representative of the receiving waters where the treated effluents of the AOPs are to be discharged [31-34].

To address the issues raised above, this study investigated fundamental and technological aspects of using novel photocatalytic materials for water treatment. Particularly, a novel supported catalyst based on nanostructured TiO_2 films deposited on a stainless steel mesh (nanoTiO$_2$-SS) by Metal Organic Chemical Vapour Deposition (MOCVD) technique was developed and tested for its performance in term of degradation of a mixture of 10 CECs present at low concentration (µg L^{-1} range). Photolytic and photocatalytic experiments were performed using groundwater as a matrix and employing a pilot scale system equipped with Hg-UV lamp ($\lambda = 254$ nm). The degradation kinetics of target contaminants and the Electrical Energy per Order (EE/O) parameter, namely the electrical energy amount that is needed for lowering the concentration of a single compound by one order of magnitude (90%) per volume unit (usually 1 m^3) of water treated [35-37] were compared with various controls including direct photolysis and photocatalysis using the conventional TiO_2 Degussa P25 catalyst. In addition, the risk of forming transformation products with higher toxicity than their parent compounds was evaluated by monitoring changes in toxicity using several acute toxicity tests covering a quite broad range of trophic levels (Microtox assay, Daphnia acute toxicity assay, Green alga Selenastrum capricornutum test, AMES mutagenic test and Fish Embryo Acute Toxicity Test) and by a preliminary investigation of the transformation products using liquid chromatography interfaced to high-resolution mass spectrometry (LC-HRMS).

2. Materials and methods

2.1 Organic pollutants and groundwater characteristics

The mixture of organic pollutants selected was defined to represent different classes of contaminants of emerging concern. It included warfarin, trimethoprim, metoprolol, carbamazepine, gemfibrozil, terbutaline, iopromide, 2,4 dihydroxy-benzophenone (BP-1), perfluorooctanesulfonic acid (PFOS), perfluorooctanoic acid (PFOA). The selected PPCPs and perfluorinated compounds (Sigma-Aldrich) along with their chemical structures and main characteristics are listed in Table S1 of the Supplementary Material.

Stock solutions were freshly prepared in groundwater spiking the target compounds to a concentration in the range of 200-400 µg L^{-1}. The groundwater collected from a well at a depth of approximately 30 m was characterized in terms of main water parameters using standard methods Table S2). It was filtered and spiked with the mixture of investigated pollutants. Solvents and chemicals (methanol and ammonium acetate) employed for both the instrumental analyses and standard solutions preparation were HPLC grade (Riedel-de Haën, Baker). A Milli-Q Gradient A-10 (Millipore) system was used for delivering ultrapure water (18.2 MΩcm, organic carbon ≤ 4µg/L) to be used for both ultra-high pressure liquid chromatography (UPLC) and standard solutions preparation. The conventional catalyst employed as a suspension for photocatalytic control experiments was Degussa (Evonik) P25 (anatase and rutile crystallites with ratio being typically 80:20, surface area 50 m^{2}g^{-1}, average diameter 30 nm).

2.2 MOCVD nanostructured TiO$_2$ film synthesis

CVD produces thin solid films from chemical precursors in the vapor phase, which are carried into a chamber containing the heated objects to be coated. Chemical reactions occur typically on heated substrates, resulting in the deposition of a thin film. This is accompanied by the production of chemical by-products that are exhausted out of the chamber along with unreacted precursor vapors.

6

When the precursor is a metal-organic compound the technique is indicated as MOCVD and permits the deposition at relatively low temperatures (i.e. 300-400°C). This technique is widely used to prepare thin films with high quality, high uniformity and controlled properties [38-39]. It offers many benefits such as high deposition rates, inherent flexibility, excellent conformal step coverage and adaptability to large scale processing also on complex substrates.

Titanium tetra-isopropoxide [Ti(O^{i}Pr)$_4$] (TTIP, 97%, where –O^{i}Pr means -OCH(CH$_3$)$_2$) was used as received (Aldrich). MOCVD experiments were carried out in a horizontal hot-wall reactor whose details and main operating parameters are reported elsewhere [40-41] that were optimized with the aim of obtaining nanostructured anatase TiO$_2$ films. The morphological and structural characteristics of the obtained coatings have been characterized by X-ray diffraction (XRD) and scanning electron microscopy (SEM). XRD patterns were measured employing a PW 3710 X-Ray diffractometer in Bragg-Brentano geometry using the Cu Kα radiation (40 kV, 30 mA, λ = 1.54056 Å). The standard patterns of the ICDD database were employed for the phase identification. Surface morphology was investigated by using a Fei Quanta 200 Field Emission Gun-Environmental Scanning Electron Microscopy (FEG-ESEM), in low vacuum mode and with acceleration voltage of 15-20 kV.

2.3 Experimental setup

A 0.5 L flow reactor equipped with a 40 W Hg low pressure UV lamp (λ=254 nm, fluence rate 50 mW cm^{-2}) was used in recirculation flow mode to perform the photolysis or photocatalytic experiments. Figure S1 shows the reactor (volume of solution treated 2 L, recirculation flow 6 L h^{-1}) used to perform the photocatalytic degradation experiments using the newly developed nanostructured TiO$_2$ supported catalysts. Three different control conditions were also tested using this setup: (i) hydrolysis (with no TiO$_2$ and UV radiation), (ii) photolysis (with UV radiation solely), (iii) photocatalysis (using TiO$_2$ P25).

Each test was carried out by placing in the reactor the freshly prepared aqueous solution of organic pollutants and sampling a first aliquot, corresponding to the time zero sample. For the UV/TiO$_2$ experiments the catalyst (50 mg L^{-1} for TiO$_2$ Degussa P25 or the stainless-steel mesh supported with TiO$_2$, TiO$_2$ loading 0.69 mg cm^{-2}, that was wrapped around the quartz tube containing the UV lamp for all its length) was then equilibrated in the dark for 30-60 min with the solution to be treated, in order to quantify the potential adsorption of the target compounds on the catalyst surface, and another aliquot was then collected. Then, the lamp was turned on and sampling was done at regular intervals over a period of 60 min. Temperature remained constant over the treatment time and pH did not change significantly likely due to the buffer capacity of the real groundwater employed (Table S2). At the end of the treatment, the photocatalyst was recovered from the aqueous solution in order to evaluate possible reuse in subsequent treatment cycles. The aqueous samples collected were centrifuged (10000 rpm x 20 min) before being placed in vials for analysis by UPLC/MS.

2.4 Toxicity tests

The toxicity tests carried out on samples collected during photolytic and photocatalytic treatments include (i) Daphnia magna Strauss (Cladocera, Crustacea) – acute toxicity tests (UNI EN ISO 6341:2013); (ii) Vibrio fischeri – test with luminescent bacteria (UNI EN ISO 11348-3:2009). The inhibition of light emission by cultures of Vibrio fischeri (NRRL B-11177) is determined by means of batch test. This is accomplished by combining specific volumes of the test sample or the diluted sample with the luminescent bacteria suspension in a test tube. The test criterion is the luminescence, measured after contact time of 30 min, taking into account of correction factor (f_{kt}), which is a measure of intensity changes of control samples during the exposure time. The amount of light emitted in the sample was used to determine the sample's relative toxicity, which can then be compared to the standard reference's toxicity. As the toxicant's concentration increases, bacterial light emissions decrease in a dose-dependent manner; (iii) Green Alga Selenastrum capricornutum

(UNI EN ISO 8692:2012). An inoculum of algal strains in exponential phase (bred for several generations in a specific medium) was placed in contact with different concentrations of the sample. The sample was diluted by mixing a suitable amount of medium to the sample itself. The batch of analysis thus prepared (algal inoculum + diluted samples) was placed to incubate for 72 ± 2 h during which the cell density was measured every 24 h. The inhibition is measured as a reduction in the kinetics of algal growth compared to the control sample. Each sample was tested with the alga *Pseudokirchneriella subcapitata*, green algae Sphaeropleales (Chlorophyta, Chlorophyceae), using the above described procedure; (iv) AMES Fluctation test (mutagenicity test) whose experimental description is reported elsewhere [42]; (v) Fish Embryo Acute Toxicity (FET) – test (OECD 236). A breeding stock of adult fish of *Danio rerio*, called "zebrafish", was maintained in glass aquaria with a continuous re-circulating system and a 14:10 h light–dark photocycle. The temperature was maintained at 26.0 ± 1.0 °C during all stages of the experiment. Adult zebrafish were fed three/four times a day with a combination of dried food and newly hatched brine shrimp of *Artemia salina*. The day before the test, an egg-trap, a glass vessel covered with a mesh, was immersed in the aquarium and it was removed at the beginning of light period after the zebrafish started spawning in order to collect the fertilised eggs. Further details of the procedure can be found elsewhere [43]. Dilution water controls are required from the guideline both as negative control and as internal plate controls as well as a positive control at a fixed concentration of 4 mg L^{-1} 3,4-dichloroaniline is been required. The test is performed in 24-well plates, 1 embryo per well was transferred inside them and distributed as following: 20 embryos per sample tested and 4 embryos for internal control. The 24-well plates were covered with lids and incubated at 26.0 ± 1.0 °C for 96 h and a light phase of 12–16 h. Every 24 h, up to four apical observations are recorded as indicators of lethality: coagulation of fertilised eggs, lack of somite formation, lack of detachment of the tail-bud from the yolk sac, and lack of heartbeat. The individual wells are considered independent replicates for statistical

9

analysis. At the end of the exposure period, acute toxicity is determined based on a positive outcome in any of the four apical observations recorded.

2.5 Chemical analysis

The residual concentration of the investigated compounds at various reaction times as well as the investigation of transformation products were carried out using a Ultimate 3000 System (Thermo Fisher Scientific) equipped with an autosampler, column over and UV detector as a chromatographic system that was interfaced to a high-resolution mass spectrometer, namely a TripleTOF® 5600+ System (AB Sciex) equipped with a duo-spray ion source that was operated in electrospray (ESI) mode in positive or negative ion mode. MS analysis was carried out by an information dependent analysis (IDA) method that includes a survey scan in TOF-MS and, after background subtraction, the isolation and fragmentation in the collision cell of the four most intense ions using parameters listed in Table S3.

The chromatography was performed using 5 µL samples injected and eluted at 0.200 mL min^{-1} through a BEH C18 column, 2.1 x 150 mm, 1.7 µm, with a binary gradient consisting of 1.5 mM ammonium in water (A) and 1.5 mM ammonium in methanol (B). The gradient started from 5 % B then was linearly increased to 95 % in 10 min and held for 7 min. At the end of each run the system was equilibrated for 5 min. Data processing was performed by MetabolitePilot 1.5, PeakView 2.2, MasterView 1.1 and MultiQuan 3.0.2 (AB Sciex).

3. Results and discussion

3.1 Nanostructured TiO$_2$/stainless steel synthesis and characterization

During the MOCVD process the deposition time is directly proportional to the thickness of the deposited film; a deposition time of 4500 s was chosen with the aim of obtaining a corresponding

TiO$_2$ film thickness of about 1500 nm. Stainless steel nets (holes of 35 μm diameter) were used as the substrate. The meshes can be uniformly covered also inside the hole walls obtaining so far a greater effective photocatalytic area. The photocatalyst is immobilized on the substrate and will not be dispersed in the testing solutions. XRD analysis of the stainless steel nets coated by TiO$_2$ indicated the formation of TiO$_2$ in the polycrystalline anatase phase (ICDD 00-021-1272) with crystallite dimension of about 30 nm calculated by the Scherrer formula (Figure S2). The surficial morphology of the film reported in Figure S3 (A) shows a typical facetted texture, while the thickness is evidenced in Figure S3 (B) with a mean value of about 1500 nm.

3.2 Direct photolysis of investigated contaminants

The photocatalytic degradation of pollutants in water matrices involves two types of reaction happening in parallel: photolysis and photocatalysis. In order to estimate the contribution of the new nanoTiO$_2$-SS catalyst in removing the target pollutants, reference experiments were conducted in presence of the light source only (photolysis experiments – absorption of radiation i.e. energy, which leads to a break-up of the compound). For each treatment tested, the reaction rate constant k (min^{-1}) was determined for each single pollutant present in aqueous matrix. The obtained values were used to determine the performance of the treatment in degrading the target pollutants and provided a comparison point for the efficiency of the newly synthesized nanoTiO$_2$-SS relative to the conventional TiO$_2$ Degussa P25 catalysts and to the photolytic treatment performed under same experimental conditions. Results reported in Figure 1a (three replicates photolytic experiments i.e. Exp1, Exp2, Exp3) showed that during photolysis performed in the 0.5 L flow reactor (Hg-UV lamp), the most recalcitrant pollutants were warfarin, trimethoprim, carbamazepine, metoprolol, and gemfibrozil with constant values in the range 0.03 min^{-1}- 0.05 min^{-1}.

11

Conversely, iopromide, terbutaline and 2,4-dihydroxybenzophenone were quickly removed by photolysis, within 5-10 minutes of treatment (Figure 1b), and the kinetics constant could not be determined. Under these treatment conditions no photolytic degradation was observed for PFOA and PFOS as shown in Figure 1b. The organic pollutants that were in a range of measurable kinetics of removal (warfarin, trimethoprim, carbamazepine, metoprolol, and gemfibrozil) were selected to determine the potential of the new nanoTiO$_2$-SS catalyst at improving the removal of CECs during photocatalytic treatment. Possible improvement for the removal of PFOS and PFOA by photocatalysis was also investigated.

3.3   Photocatalytic removal of CECs

The degradation kinetics of the investigated mixture of CECs in groundwater followed the model of Langmuir-Hinshelwood showing first-order kinetics for all the investigated contaminants (data not shown). Figure 2 shows the first-order kinetic constants obtained during photocatalytic treatments of CECs employing nanoTiO$_2$-SS, conventional suspended catalysts TiO$_2$ Degussa P25 (50 mg L^{-1}) and photolytic treatment. No measurable removals were observed, under all conditions, for PFOS and PFOA. Control experiments performed in the dark (data not shown) and in the presence of catalysts indicated that the amount of CECs adsorbed on the catalyst was negligible. Such a finding also demonstrated any possible hydrolysis of the target pollutants due to the catalysts did not occur. According to the results shown in Figure 2, the nanoTiO$_2$-SS demonstrated a better performance in degrading the target pollutants in groundwater when compared to photolysis and photocatalysis using conventional TiO$_2$. The performance of the new catalyst significantly surpassed the TiO$_2$ Degussa P25 despite the fact that the active surface of a catalyst is reduced once deposited onto a surface. The ratio between the calculated kinetic constants $k_{nanoTiO2-SS}/k_{TiO2\ DegP25}$ indicated that the rate of removal of warfarin and trimethoprim obtained with the new catalyst was twice the one observed using TiO$_2$ Degussa P25 and approximately 1.6 times faster for metoprolol,

12

carbamazepine and gemfibrozil. At the end of each photocatalytic treatment it was possible to recovery the supported catalyst from the UV reactor and to reuse the same for further treatments without large losses in term of performance degradation. Specifically, after ten reactions the performance of the catalyst was in the range 75-90 % depending of the organic pollutant.

3.4   Energy requirement for the removal of CECs

From the degradation profiles of each investigated organic contaminants as a function of the UV dose applied, the Electrical Energy per Order or EE/O parameter (kWh/m^3) was calculated using the following equation [35-37]:

$$UVdose(kWh/m^3) = EE/O \; x \log(Ci/Cf)$$

where C_i and C_f are the initial and final pollutant concentrations, respectively. The UV dose parameter combines flow rate, residence time and light intensity into a single term given by the following expression:

$$UVdose(kWh/m^3) = \frac{1000 \; x \; UV \; power \; (kW) \; x \; t \; (min)}{60 \; x \; V \; (L)}$$

where V is the volume (L) of the treated water. From these two equations, and knowing the kinetic expression of the reaction rate *ln (C_i/C_f) = k t*, EE/O can be defined or calculated as follows:

$$EE/O(kWh/m^3) = \frac{38.4 \; x \; UV \; power \; (kW)}{V \; (L) \; x \; k \; (min^{-1})}$$

13

where k is the first-order-rate constant (min^{-1}) for the disappearance or degradation of the target pollutant concentration. Comparing the EE/O values obtained for photolysis and photocatalysis reactions (Table 1) indicated that photocatalysis treatment employing the nanoTiO$_2$-SS significantly lowered the energy requirement for a given removal for all the emerging organic pollutants tested (24.3-31.8 kWh m^{-3} rather than 49.6-129 kWh m^{-3}).

These results confirm the improved performance offered by the nanoTiO$_2$-SS using another evaluation criteria, the electrical energy per order of degradation commonly used in the water treatment industry to compare different UV-based technologies, and further indicate the that the performance in degrading target pollutants is compound-dependent. Using trimethoprim as an example, it is possible to conclude that photocatalysis had an EE/O value (28.7 kWh m^{-3}) almost five times lower that for photoloysis (120 kWh m^{-3}).

3.5 Evaluation of toxicity screening of treated water

To further evaluate the efficiency of treatment, toxicity tests were performed on samples collected during treatment using nanoTiO$_2$-SS and control conditions (photolysis and photocatalysis using Degussa P25) at set reaction times of 0 min, 7.5 min and 60 min and for the following. All treatments were performed in duplicates and the results of toxicity tests represent an average of the values obtained performing the specific test on both replicates for each investigated reaction time and treatment type.

Table 2 summarizes the results obtained from the acute toxicity tests performed with *Daphnia magna Strauss, Vibrio fischeri and Green Alga Selenastrum Capricornutum* as well as the AMES Fluctation test. As for the determination of the inhibition of the mobility of *Daphnia Magna Straus* (UNI EN ISO 6341:2013), expressed as % of mobility inhibition, considering that a 10% of mobility inhibition is considered as non-toxic, the results indicated that the initial solution was not

14

toxic based on this assay and that all the investigated treatments did not increase the toxicity of treated solutions. The effects might have been lower than the limit of detection of the assays.

The *Vibrio fischeri* results (UNI EN ISO 11448-3:2009) (Table 2) are expressed as percentage of bioluminescence inhibition for the target bacteria. The limit test described in the UNI EN ISO 11348-3 expected that samples showing a bioluminescence inhibition less than 20% are non-toxic. The percentage of inhibition of bioluminescence was less than 20% in the sample collected at time 0 and in all samples treated for 60 min. However, some transient increase in the toxicity, to level barely above the limit of non-toxic effect, 23.7% and 21.5%, were observed for samples collected during photocatalytic treatments in presence of the nanoTiO$_2$-SS and the conventional TiO$_2$ Degussa P25, respectively.

The results obtained using the more sensitive toxicity test, i.e. Green Alga Selenastrum capricornutum test (UNI EN ISO 8692:2012), revealed that there was a decrease in toxicity after 60 minutes of reaction for all the investigated treatments. As for AMES Fluctation test the results summarized in Table 8 are expressed as a mutagenicity ratio (MR= number of positive wells in samples/number of positive wells in the negative control). Statistical significance that occurred in the number of positive wells compared with spontaneous revertant wells was determined using the chi-square (χ^2) analysis [44]. According to the results in Table 2, all the samples demonstrated a mutagenic effect. While a decrease in toxicity was observed after 60 min of reaction for the photocatalytic treatment in presence of the supported TiO$_2$ on stainless steel (MR=2.5), increase mutagenicity was observed for the same treatment after 7.5 min.

Finally, as for the fish embryo acute toxicity (FET) test (OECD 236) all the validity conditions of test were respected: fertilization eggs $\geq$ 70%, survival rate and hatching rate in the negative control were respectively $\leq$ 90% and $\geq$ 80% at 96 h, the mortality in the positive control DCA 4 mg L^{-1} was $\geq$ 30% at 96 h. Daily cumulative lethal percentages for the two replicates are listed in Table 3.

15

The results showed for the embryos of *Danio rerio* an initial toxicity (prior to treatment, time 0 min), 55 % for replicate 1 and 40-45 % for replicate 2. During the times of exposure the toxicity seems to remain quite the same for the three treatments, with a maximum increment of 15 % at 7.5 min for photolysis (Figure 3). To better understand the results reported in Table 3, the average values of lethal effect obtained from the two replicates for each performed treatment (at 7.5 min and 60 min) were plotted in Figure 3 for comparison with the initial effect i.e. 0 min (dashed line).

Table 4 presents the percentages of lethal effect calculated at 96 h for the three different treatments. In addition to the previous evaluation, the OECD Guideline recommends also to note and report any secondary effects of embryo abnormalities at the end of the tests; particular relevance should be given to the hatching of eggs. The eggs exposed to samples collected during photolysis and photocatalysis with conventional Degussa P25 showed a significant delay in hatching (Table 4) at the time points 7.5 min and 60 min. Only the treatment with nanoTiO$_2$-SS mesh allowed the normal development of embryos and the hatching of eggs in time.

Overall, toxicity results evidenced that the AMES Fluctuation Test and Fish Embryo Acute Toxicity (FET) gave similar results for the treated groundwater samples, namely a slight increase at 7.5 min and then a decrease at 60 min, while test Growth Inhibition test (Green Alga) showed a continuous decrease in toxicity during all the investigated treatment times. Instead, *Daphnia Magna Straus* and Vibrio tests were not sensitive enough to the investigated samples.

3.6   Identification of degradation products

Identification of degradation products was mainly performed aimed at verifying whether the photocatalytic process carried out with the nanoTiO$_2$-SS catalyst led to different compounds with respect to the reaction performed with the conventional Degussa P25 catalyst. Accordingly, identification of degradation products was only focused to the most abundant compounds present in the reaction mixtures. Indeed, the complete identification of degradation products formed is a very

difficult tasks mainly due to the fact that the reactions were performed with a real water matrix (groundwater) and with a mixture of ten CECs. Main identified degradation products are listed in Table 5. For each of them the assignment of elemental composition was made possible by combining high-resolution mass spectrometry data with the information contained in high-resolution mass spectra about the isotopic distribution of ions, defined as spectral accuracy [45]. In addition, for 9 out of 12 compounds on the basis of the information obtained in single and in tandem high resolution MS mode it was also possible to propose a chemical structure derived from one of the parent compounds included in the mixture. Results listed in Table 5 show that the main identified degradation products derived from five (Terbutaline, Warfarin, Trimethoprim, BP-1, Metoprolol) out eight pollutants that showed to be degraded (PFOS and PFOA were not degraded). Such degradation products were mainly formed due to oxidation reaction, namely inserting a hydroxyl group on the aromatic ring, as well as to further reaction leading to a breakdown of the structure of parent compounds. No degradation products coming from carbamazepine, Gemfibrozil and iopromide were identified. This could be inferred to the higher reactivity of these compounds leading quite quikly to breakdown products that were high polar and thus not amenable to be analyzed by UPLC method employed. The detected degradtion products also showed to follow different formation/degradtion profiles (Figure S4). Specifically, some of the follow a typical bell-shape trend while others were constantly formed during the investigated reaction time. Table 5 also show that the identified degradation products were not detected during all reactions. It follows that minor differences were found between photocatalysis performed with nanoTiO$_2$-SS and Degussa P25 catalysts suggesting also minor differences in the reaction mechanism. However, further investigation must be performed to demonstrate such a finding.

17

4. Conclusions

The employment of a new supported catalyst based on nanostructured TiO_2 films deposited on a stainless steel mesh (nanoTiO2-SS) for the photocatalytic degradation of a mixture of contaminants of emerging concern in real groundwater revealed a better performance than the conventional Degussa P25 catalyst. The supported catalyst was active after several cycles of photocatalytic treatments demonstrating the possibility to be conveniently re-used for several subsequent photocatalytic treatments. The evaluation of the electrical energy per order magnitude of removal (EE/O) confirmed the better performance of the new catalyst with respect to Degussa P25 and that the performance in degrading the target pollutants is compound-dependent. Toxicity tests revealed that some of them are really worth to be used for investigation of environmental effects of treated waters containing contaminants of emerging concern at $\mu g \ L^{-1}$ level. Specifically, AMES Fluctuation Test, Fish Embryo Acute Toxicity and Growth Inhibition test by Green Alga were able to provide valuable results for an environmental assessment. On the other hand, *Daphnia Magna Straus* and Vibrio tests were not sensitive enough to the investigated samples. Overall, results showed that the integration of both the chemical and toxicological analysis provides a powerful tool for determining the potential hazards associated with contaminants of emerging concern.

18

References

[1] N. Ratola, A. Cincinelli, A. Alves, A. Katsoyiannis, Occurrence of organic microcontaminants in the wastewater treatment process. A mini review. *Journal of Hazardous Materials* 239–240 (2012) 1-18.

[2] Y. Luo, W. Guo, H.H. Ngo, L.D Nghiem, F.I. Hai, J. Zhang, S. Liang, X.C. Wang. A review on the occurrence of micropollutants in the aquatic environment and their fate and removal during wastewater treatment. *Science of Total Environment* 473–474 (2014), 619–641.

[3] E.Z. Harrison, S.R. Oakes, M. Hysell, A. Hay. Organic chemicals in sewage sludges. *Science of Total Environment.* 367 (2006) 481-497.

[4] A. Jurado, E. Vazquez-Sune, J. Carrera, M. Lopez de Alda, E. Pujades, D. Barcelo. Emerging organic contaminants in groundwater in Spain: a review of sources, recent occurrence and fate in a European context. *Science of Total Environment* 440 (2012), 82–94.

[5] C.A. Kinney, E.T. Furlong, S.D. Zaugg, M.R. Burkhardt, S.L. Werner, J.D. Cahill, G.R. Jorgensen, Survey of Organic Wastewater Contaminants in Biosolids Destined for Land Application, *Environment Science Technology* 40 (2006) 7207-7215.

[6] E.K. Muirhead, A.D. Skillman, S.E. Hook, I.R. Schultz, Oral Exposure of PBDE-47 in Fish: Toxicokinetics and Reproductive Effects in Japanese Medaka (Oryzias latipes) and Fathead Minnows (Pimephales promelas), *Environment Science Technology* 40 (2005) 523-528.

[7] M. DeLorenzo, J. Fleming, Individual and Mixture Effects of Selected Pharmaceuticals and Personal Care Products on the Marine Phytoplankton Species Dunaliella tertiolecta, *Arch. Environ. Contam. Toxicol.* 54 (2008) 203-210.

[8] J.E. Drewes, S. Khan, Water Reuse for Drinking Water Augmentation, in: J. Edzwald, (Ed.), *Water Quality and Treatment*, 6th Edition, American Water Works Association, Denver, Colorado. 2011, pp. 48.

[9] A. R. Ribeiro, O. C. Nunes, M. F. R. Pereira, A. M. T. Silva. An overview on the advanced oxidation processes applied for the treatment of water pollutants defined in the recently launched Directive 2013/39/EU. *Environment International* 75 (2015) 33–51.

[10] I. Muñoz, S. Malato, A. Rodríguez, X. Domènech. Integration of Environmental and Economic Performance of Processes. Case Study on Advanced Oxidation Processes for Wastewater Treatment. *J. Adv. Oxid. Technol.* 11 (2008) 270-275.

[11] M. Klavarioti, D. Mantzavinos, D. Kassinos. Removal of residual pharmaceuticals from aqueous systems by advanced oxidation processes. *Environment International* 35 (2009) 402–417.

[12] S. W. da Silvaa, C. R. Klauckb, M. A. Siqueirab, A. M. Bernardesa. Degradation of the commercial surfactant nonylphenol ethoxylate by advanced oxidation processes. *Journal of Hazardous Materials* 282 (2015) 241–248

[13] A. Asghar, A. A. Abdul Raman, Wan Mohd Ashri Wan Daud. Advanced oxidation processes for in-situ production of hydrogen peroxide/hydroxyl radical for textile wastewater treatment: a review. *Journal of Cleaner Production* 87 (2015) 826-838.

[14] J.L. de Morais, P.P. Zamora. Use of advanced oxidation processes to improve the biodegradability of mature landfill leachates. *Journal of Hazardous Materials* 123 (2005) 181-186.

[15] I. Oller, S. Malato, J.A. Sánchez-Pérez. Combination of Advanced Oxidation Processes and biological treatments for wastewater decontamination ‐ A review. *Science of the Total Environment* 409 (2011) 4141–4166.

[16] A. Bernabeu, R.F. Vercher, L. Santos-Juanes, P.J. Simón, C. Lardín, M.A. Martínez, J.A. Vicente, R. González, C. Llosá, A. Arques, A.M. Amat, Solar photocatalysis as a tertiary treatment to remove emerging pollutants from wastewater treatment plant effluents, Catal. Today 161 (2011) 235-240.

20

[17] L.F. Gonzalez, V. Sarria, O.F. Sanchez. "Degradation of chlorophenols by sequential biological-advanced oxidative process using Trametes pubescens and TiO_2/UV". *Bioresource Technology* 101 (2010), 3493–3499.

[18] C. Di Iaconi, G. Del Moro, M. De Sanctis, S. Rossetti, A chemically enhanced biological process for lowering operative costs and solid residues of industrial recalcitrant wastewater treatment, Water Res. 44 (2010) 3635-3644.

[19] M.A. Sousa, C. Gonçalves, V.J.P. Vilar, R.A.R. Boaventura, M.F. Alpendurada, Suspended TiO_2-assisted photocatalytic degradation of emerging contaminants in a municipal WWTP effluent using a solar pilot plant with CPCs, Chem. Eng. J. 198–199 (2012) 301-309.

[20] M.N. Sugihara, D. Moeller, T. Paul, T.J. Strathmann, TiO_2-photocatalyzed transformation of the recalcitrant X-ray contrast agent diatrizoate, Appl. Catal. B-Environ. 129 (2013) 114-122.

[21] L. Prieto-Rodriguez, S. Miralles-Cuevas, I. Oller, A. Agüera, G.L. Puma, S. Malato, Treatment of emerging contaminants in wastewater treatment plants (WWTP) effluents by solar photocatalysis using low TiO_2 concentrations, J. Hazard. Mater. 211–212 (2012) 131-137.

[22] J. A. Dumesic, G. W. Huber, M. Boudart. Principles of Heterogeneous Catalysis, Handbook of Heterogeneous Catalysis, Part 1. Introduction (2008).

[23] M. Pelaez, N.T. Nolan, S.C. Pillai, M.K. Seery, P. Falaras, A.G. Kontos, P.S.M. Dunlop, J.W.J. Hamilton, J.A. Byrne, K. O'Shea, M.H. Entezari, D.D. Dionysiou, A review on the visible light active titanium dioxide photocatalysts for environmental applications, Appl. Catal. B-Environ. 125 (2012) 331-349.

[24] R. Comparelli, E. Fanizza, M.L. Curri, P.D. Cozzoli, G. Mascolo, A. Agostiano, UV-induced photocatalytic degradation of azo dyes by organic-capped ZnO nanocrystals immobilized onto substrates, Appl. Catal. B-Environ. 60 (2005) 1-11.

[25] N. Miranda-García, S. Suárez, B. Sánchez, J.M. Coronado, S. Malato, M.I. Maldonado, Photocatalytic degradation of emerging contaminants in municipal wastewater treatment plant effluents using immobilized TiO_2 in a solar pilot plant, Appl. Catal. B-Environ. 103 (2011) 294-301.

[26] G. Mascolo, R. Comparelli, M.L. Curri, G. Lovecchio, A. Lopez, A. Agostiano, Photocatalytic degradation of methyl red by TiO_2: Comparison of the efficiency of immobilized nanoparticles versus conventional suspended catalyst, J. Hazard. Mater. 142 (2007) 130-137.

[27] R. Leary, A. Westwood, Carbonaceous nanomaterials for the enhancement of TiO_2 photocatalysis, Carbon 49 (2011) 741-772.

[28] S. Murgolo, F. Petronella, R. Ciannarella, R. Comparelli, A. Agostiano, M.L. Curri, G. Mascolo. UV and solar-based photocatalytic degradation of organic pollutants by nano-sized TiO_2 grown on carbon nanotubes. *Catalysis Today* 240 (2015), 114-124.

[29] D. Fatta-Kassinos, M.I. Vasquez, K. Kümmerer. Transformation products of pharmaceuticals in surface waters and wastewater formed during photolysis and advanced oxidation processes – Degradation, elucidation of byproducts and assessment of their biological potency *Chemosphere* 85 (2011) 693–709.

[30] A. Agüera & M. Jesús Martínez Bueno & A. R. Fernández-Alba. New trends in the analytical determination of emerging contaminants and their transformation products in environmental waters. *Environ Sci Pollut Res* 20 (2013), 3496–3515.

[31] J. C. Cardoso da Silva, J. A. Reis Teodoro, R. J. de Cássia Franco Afonso, S.F. Aquino and R. Augusti. Photolysis and photocatalysis of ibuprofen in aqueous medium: characterization of byproducts via liquid chromatography coupled to high-resolution mass spectrometry and assessment of their toxicities against Artemia Salina. *Journal of mass spectrometry* 49 (2014), 145–153.

22

[32] D. Nasuhoglu, V. Yargeau, D. Berk**.** Photo-removal of sulfamethoxazole (SMX) by photolytic and photocatalytic processes in a batch reactor under UV-C radiation ($\lambda_{max} = 254$ nm). *Journal of Hazardous Materials* 186 (2011) 67–75.

[33] K. Barbusiński. Toxicity of Industrial Wastewater Treated by Fenton's Reagent. *Polish Journal of Environmental Studies* Vol. 14, No. 1 (2005), 11-16.

[34] R. Andreozzi, R. Marotta, G. Pinto, A. Pollio. "Carbamazepine in water: persistence in the environment, ozonation treatment and preliminary assessment on algal toxicity" *Water Research* 36 (2002), Issue 11, 2869–2877.

[35] G. Mascolo, R. Ciannarella, L. Balest, A. Lopez. Effectiveness of UV based advanced oxidation processes for the remediation of hydrocarbon pollution in the groundwater: A laboratory investigation. *Journal of Hazardous Materials* 152 (2008), 1138-1145.

[36] N. Daneshvar, A. Aleboyeh, A.R. Khataee. The evaluation of electrical energy per order (EEo) for photooxidative decolorization of four textile dye solutions by the kinetic model. *Chemosphere* 59 (2005), 761–767.

[37] AOT Handbook, Calgon Carbon Corporation. Markham, Ontario; Tucson, Arizona; Pittsburgh, PA (1996).

[38] A. Devi, 'Old Chemistries' for new applications: Perspectives for development of precursors for MOCVD and ALD applications, Coordination Chemistry Reviews, 257 (2013) 3332–3384

[39] A. C. Jones and Mi L. Hitchman, Chemical Vapour Deposition: Precursors, Processes and Applications, Edited by Anthony C. Jones and Michael L. Hitchman, published by the Royal Society of Chemistry (2009).

[40] R. Gerbasi, M. Bolzan, N. El Habra, G. Rossetto, L. Schiavi, A. Strini, S. Barison. Photocatalytic Activity Dependence on the Structural Orientation of MOCVD TiO_2 Anatase Films, J. Electrochem. Soc. 156(12) (2009) K233-K237.

23

[41] S. Battiston, M. Minnella, R. Gerbasi, F. Visentin, P. Guerriero, A. Leto, G. Pezzotti, E. Miorin, M. Fabrizio, C. Pagura, Growth of titanium dioxide nanopetals induced by single wall carbon nanohorns, Carbon 48(9) (2010), 2470-2477.

[42] E. Ubomba-Jaswa, P. Fernandez-Ibanez, K. G. McGuigan. A preliminary Ames fluctuation assay assessment of the genotoxicity of drinking water that has been solar disinfected in polyethylene terephthalate (PET) bottles. Journal of Water and Health, 8(4) (2010), 712-718.

[43] F. Busquet, R. Strecker, J. M. Rawlings, S. E. Belanger, T. Braunbeck, G. J. Carr, P. Cenijn, P. Fochtman, A. Gourmelon, N. Hubler, A. Kleensang, M. Knobel, C. Kussatz, J. Legler, A. Lillicrap, F. Martinez-Jeronimo, C. Polleichtner, H. Rzodeczko, E. Salinasm, K. E. Schneiderm, S. Scholz, E. J. van den Brandhof, L. T. M. van der Ven, S. Walter-Rohde, S. Weigt, H. Witters, M. Halder. OECD validation study to assess intra- and inter-laboratory reproducibility of the zebrafish embryo toxicity test for acute aquatic toxicity testing. Regulatory Toxicology and Pharmacology 69 (2014) 496-511.

[44] R. I. Gilbert. The analysis of fluctuation test. Mutation Research 74 (4) (1980), 283-289.

[45] A. Amorisco, V. Locaputo, C. Pastore, G. Mascolo. Identification of low molecular weight organic acids by ion chromatography/hybrid quadrupole time-of-flight mass spectrometry during Uniblu-A ozonation. Rapid Commun. Mass Spectrom. (2013), 27, 187-199.

Figure 1.   (a). First order kinetic constants (k) of UV photolytic treatments for removal of investigated organic pollutants in groundwater employing the flow UV. Three replicates used: Exp 1, Exp 2 and Exp 3. (b). Photolytic degradation of iopromide, terbutaline, BP-1, PFOA and PFOS in groundwater employing the flow UV reactor (light source 40 W Hg lamp, reactor volume: 0.5 L, treated volume: 2 L, recirculation flow rate: 6 L h^{-1}).

Figure 2.   Photocatalytic performance of TiO_2 supported catalyst on stainless steel as compared to photolysis and conventional Degussa P25 for the removal of target emerging pollutants in groundwater (light source 40W Hg lamp, reactor volume: 0.5 L, treated volume: 2 L, recirculation flow rate: 6 L h^{-1}). Error bars = 1 standard deviation of three replicates.

Figure 3.   Comparison of the averages of lethal effect of the different reaction with the initial effect.

Table 1. EE/O values obtained for the degradation of CECs in groundwater employing the flow UV reactor operated for photolysis and photocatalysis.

	Electrical Energy per Order of degradation (EE/O) [kWh m^{-3}]		
	Photolysis	Photocatalysis, TiO$_2$ Degussa P25	Photocatalysis, nanoTiO$_2$-SS
Trimethoprim	129	59.5	28.7
Metoprolol	60.5	39.4	24.3
Carbamazepine	116	52.2	31.8
Gemfibrozil	78.1	47.8	28.4
Warfarin	93.1	49.6	25.1

Table 2. Acute toxicity tests performed with Daphnia magna Strauss, Vibrio fischeri, Green Alga Selenastrum Capricornutum and AMES Fluctation test.

	Daphnia magna Strauss *(% Mobility inhibition)*	*Vibrio fischeri* (% Bioluminescence inibition)	*Green Alga Selenastrum capricornutum* (% Growth Inibition)	AMES Fluctation test (*Mutagenicity Ratio*, *MR)*
Reaction time = 0 min	< 10	< 20	53.2	3.9
Photocatalysis, nanoTiO$_2$-SS				
Reaction time = 7.5 min	< 10	23.7	45.9	5.3
Reaction time = 60 min	< 10	< 20	25.7	2.5
Photolysis				
Reaction time = 7.5 min	< 10	< 20	48.3	4.4
Reaction time = 60 min	< 10	< 20	27.2	4.7
Photocatalysis, conventional TiO$_2$ Degussa P25				
Reaction time = 7.5 min	< 10	21.5	49.8	5.2
Reaction time = 60 min	< 10	< 20	23.4	6.4

27

Table 3. Cumulative mortality percentages based on daily apical observation for four days of observation.
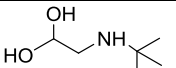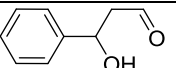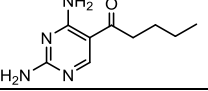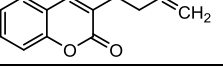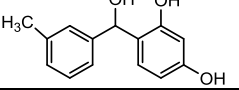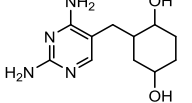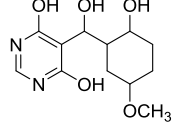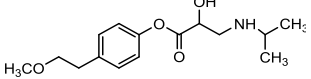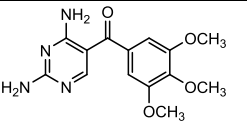
	Day1	Day 2	Day 3	Day 4
Control ISO	0%	0%	0%	0%
3,4 DCA 4mg L^{-1} ISO	0%	40%	70%	70%
Replicate 1				
Reaction time = 0 min	55%	55%	55%	55%
Photocatalysis, nanoTiO$_2$-SS Reaction time = 7.5 min	35%	35%	40%	45%
Photocatalysis, nanoTiO$_2$-SS Reaction time = 60 min	40%	45%	50%	50%
Photolysis, UV Reaction time = 7.5 min	50%	50%	55%	60%
Photolysis, UV Reaction time = 60 min	55%	55%	55%	55%
Photocatalysis, TiO$_2$ DegP25 Reaction time = 7.5 min	50%	65%	65%	65%
Photocatalysis, TiO$_2$ DegP25 Reaction time = 60 min	50%	55%	60%	60%
Replicate 2				
Reaction time = 0 min	40%	45%	45%	45%
Photocatalysis, nanoTiO$_2$-SS Reaction time = 7.5 min	50%	55%	60%	60%
Photocatalysis, nanoTiO$_2$-SS Reaction time = 60 min	65%	70%	70%	70%
Photolysis, UV Reaction time = 7.5 min	65%	70%	70%	70%
Photolysis, UV Reaction time = 60 min	65%	70%	70%	70%
Photocatalysis, TiO$_2$ DegP25 Reaction time = 7.5 min	40%	45%	45%	45%
Photocatalysis, TiO$_2$ DegP25 Reaction time = 60 min	55%	55%	55%	55%

Table 4. Percentages of lethal effect calculated at 96 hours for the three different treatments.

	Photolysis	Photocatalysis, nanoTiO$_2$-SS	Photocatalysis, conventional TiO$_2$ Degussa P25
Reaction time = 0 min	50%	50%	50%
Reaction time = 7.5 min	65%*	53%	55%*
Reaction time = 60 min	63%*	60%	58%*

*secondary observation of abnormalities, delay of hatching.

Table 5. Degradation products identified during the degradation of a mixture of contaminants of emerging concern in real groundwater by photolysis and photocatalysis using both Degussa P25 and a stainless steel mesh (nanoTiO₂-SS) catalyst.

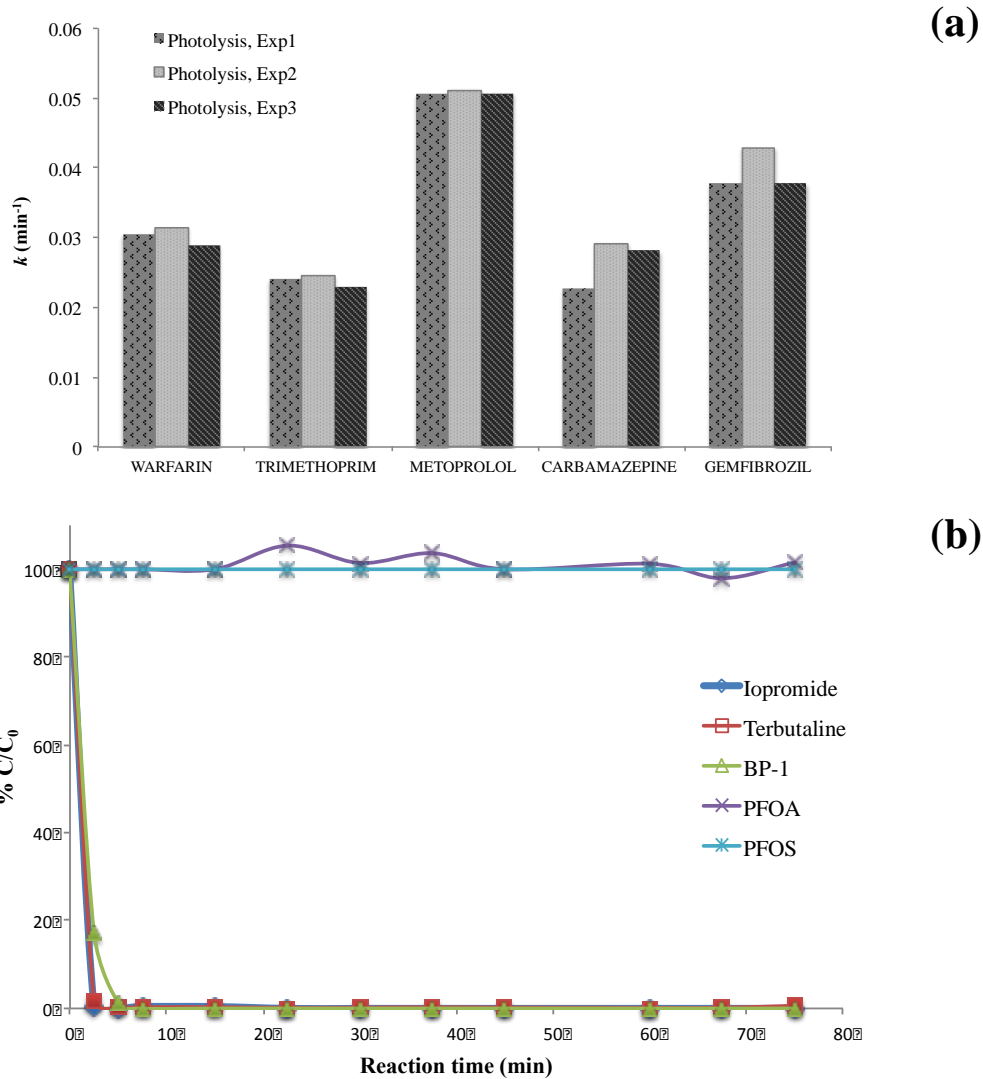|	Measured mass, [M+H]$^+$ (m/z)	Calculated mass (m/z), [M+H]$^+$ (m/z)	Formula	RT (min)	Proposed structure	Parent compound	Identified during reaction with		
							UV	UV/ P25	UV/ nanoTiO₂-SS
TP1	134.1173	134.1176	$C_6H_{15}NO_2$	2.5		Terbutaline	X	X	X
TP2	151.0958	151.0754	$C_9H_{10}O_2$	4.2		Warfarin			X
TP3	195.1240	195.1240	$C_9H_{14}N_4O$	4.9		Trimethoprim			X
TP4	201.0904	201.0910	$C_{13}H_{12}O_2$	11.4		Warfarin	X	X	X
TP5	231.1016	231.1016	$C_{14}H_{14}O_3$	9.1		BP-1		X	X
TP6	239.1503	239.1502	$C_{11}H_{18}N_4O_2$	5.5		Trimethoprim		X	X
TP7	271.1288	271.1289	$C_{12}H_{18}N_2O_5$	6.2		Trimethoprim		X	X
TP8	282.1700	282.1699	$C_{15}H_{23}NO_4$	8		Metoprolol	X	X	X
TP9	295.1387	295.1387	$C_{12}H_{22}O_8$	6.3			X	X	X
TP10	305.1233	305.1244	$C_{14}H_{16}N_4O_4$	8.5		Trimethoprim	X	X	X
TP11	367.3301	367.3319	$C_{22}H_{42}N_2O_2$	12.1			X	X	
TP12	425.3829	425.3850	$C_{24}H_{48}N_4O_2$	12.1			X	X	

Figure 1

(a)

(b)

Figure 1. (a). First order kinetic constants (k) of UV photolytic treatments for removal of investigated organic pollutants in groundwater employing the flow UV. Three replicates used: Exp 1, Exp 2 and Exp 3. (b). Photolytic degradation of iopromide, terbutaline, BP-1, PFOA and PFOS in groundwater employing the flow UV reactor (light source 40 W Hg lamp, reactor volume: 0.5 L, treated volume: 2 L, recirculation flow rate: 6 L h^{-1}).
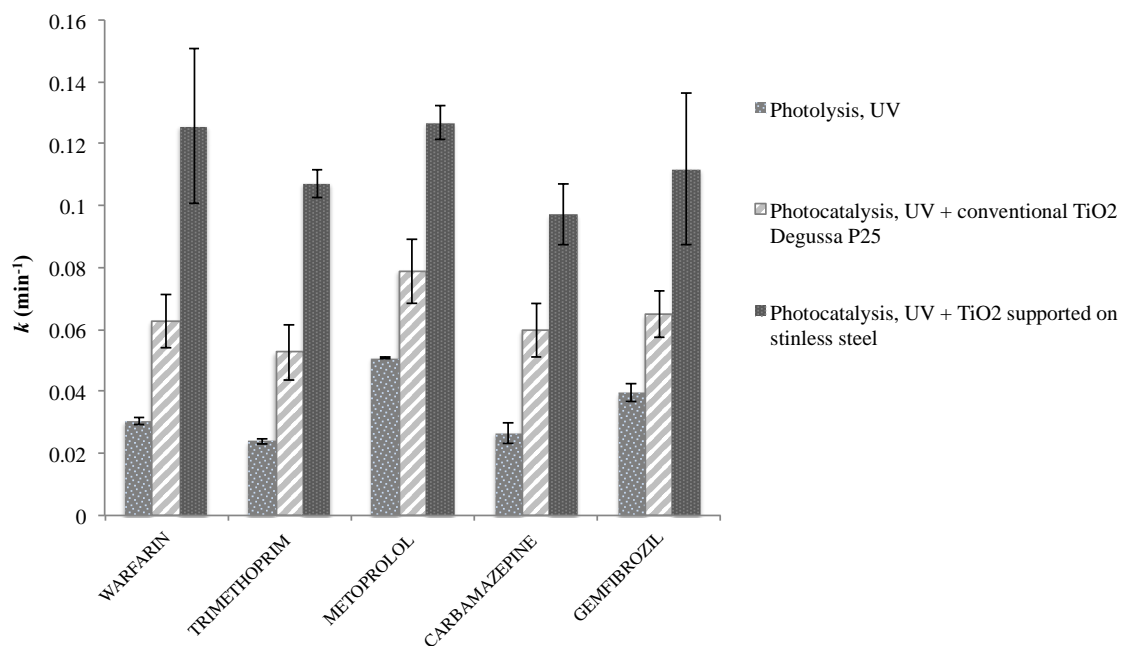
Figure 2

Figure 2. Photocatalytic performance of TiO$_2$ supported catalyst on stainless steel as compared to photolysis and conventional Degussa P25 for the removal of target emerging pollutants in groundwater (light source 40W Hg lamp, reactor volume: 0.5 L, treated volume: 2 L, recirculation flow rate: 6 L h^{-1}). Error bars = 1 standard deviation of three replicates.
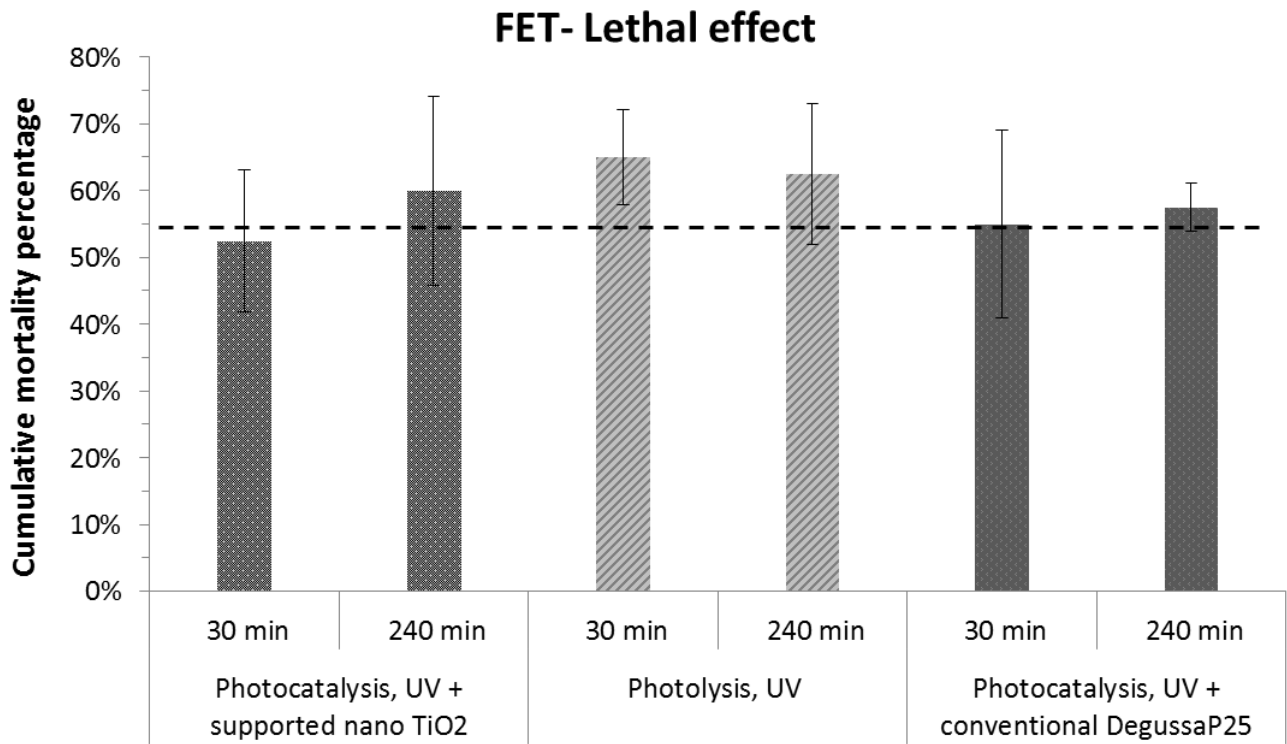
Figure 3

Figure 3. Comparison of the averages of lethal effect of the different reaction with the initial effect.

Supplementary Material